PHYSICAL REVIEW D **96,** 016001 (2017)

Compact Q-balls and Q-shells in CP^N-type models

P. Klimas[1] and L. R. Livramento[1,2]

[1]*Departamento de Física, Universidade Federal de Santa Catarina, Campus Trindade, CEP 88040-900 Florianópolis-SC, Brazil*

[2]*Instituto de Física de São Carlos; IFSC, Universidade de São Paulo, Caixa Postal 369, CEP 13560-970 São Carlos-SP, Brazil*

(Received 14 April 2017; published 5 July 2017)

We show that the CP^N model with an odd number of scalar fields and a V-shaped potential possesses some finite energy compact solutions in the form of Q-balls and Q-shells. Such solutions were obtained in $3+1$ dimensions. The Q-balls appear for $N=1$ and $N=3$, whereas the Q-shells are present for higher odd numbers N. We show that the energy of the solutions behaves as $E \sim |Q|^{5/6}$, where Q stands for the Noether charge.

DOI: 10.1103/PhysRevD.96.016001

I. INTRODUCTION

Field-theoretic models that admit soliton solutions became popular in many branches of physics such as cosmology, particle physics, nuclear physics, and condensed matter physics. Solitons are very special stable field configurations whose properties are related to conserved quantities. They are usually studied as solutions of some effective classical nonlinear field models which are expected to grasp the most relevant physical properties of the underlying quantum theory. For instance, the Skyrme model and the Skyrme-Faddeev (SF) model together with their extensions are intensively studied in the context of a description of nuclear matter and strong interactions [1].

Another important group of field-theoretic models is formed by the CP^N models, i.e., models on a complex projective space [2]. The CP^N models have a close relation with so-called nonlinear sigma models which have applications in diverse areas of physics. For instance, the simplest one in this group, the CP^1 model, is related to the model describing the Heisenberg ferromagnet [3], and it is defined by the Lagrangian $\mathcal{L}_0 = \frac{1}{2}\partial_\mu\vec{\phi}\cdot\partial^\mu\vec{\phi}$, where the triplet of real scalar fields $\vec{\phi} = (\phi^1, \phi^2, \phi^3)$ satisfies the constraint $\vec{\phi}\cdot\vec{\phi} = 1$. The relation between the nonlinear sigma model and the CP^1 model is established by the stereographic projection. An important point about the Lagrangian $\mathcal{L}_0$ is that it appears as a part of the Lagrangians of the Skyrme model [defined in terms of $\vec{\phi} \in S^2$ instead of chiral fields $U \in SU(2)$] and of the SF model. The general CP^N model is defined by the Lagrangian $\mathcal{L}_{CPN} = \lambda^2 (D_\mu \mathcal{Z})^\dagger D^\mu \mathcal{Z}$, where λ^2 is a dimensional constant and $D_\mu \mathcal{Z} \equiv \partial_\mu \mathcal{Z} - (\mathcal{Z}^\dagger\cdot\partial_\mu \mathcal{Z})\mathcal{Z}$. The vector $\mathcal{Z}$ has the form $\mathcal{Z} = (\mathcal{Z}_1, \ldots, \mathcal{Z}_{N+1})$ and satisfies the constraint $\mathcal{Z}^\dagger \mathcal{Z} = 1$. A set of independent complex fields is introduced as $\mathcal{Z} = (u_1, \ldots, u_N, 1)/\sqrt{1+u^\dagger\cdot u}$. Some more complex models contain the CP^N Lagrangian as one of the terms in a total action. For instance, it takes place for the extended SF model with a target space $SU(N+1)/SU(N)\otimes U(1) = CP^N$; see [4].

The existence of topological solutions of the CP^N models is closely related to the homotopy classes $\pi_k(CP^N)$, where k is a dimension of the base space. According to Ref. [5], the $k=2$ planar models on a coset space G/H possess the homotopy class $\pi_2(CP^N) = \pi_1(H)_G$, where $\pi_1(H)_G$ is a subset of $\pi_1(H)$ formed by closed paths in H which can be contracted to a point in G. It follows that topological charges of the CP^N model are given by $\pi_1(SU(N)\otimes U(1))_{SU(N+1)}$ and they are equal to the number of poles of u_i (including those at infinity). It has been shown that the CP^N model and the extended SF model with the CP^N target space possess exact topological vortex solutions [4,6] and numerical vortex solutions in the models containing a potential term [7]. Although such vortices were obtained in $3+1$ dimensions, their topological charge density and the energy density are functions of merely two spatial coordinates. Unfortunately, there are no corresponding solutions for $k=3$ and $N>1$, because the homotopy class $\pi_3(CP^N)$ is trivial [note that $\pi_3(CP^1) = Z$]. It leads to the conclusion that models in three spatial dimensions with the CP^N target space, where $N>1$, can have only nontopological solutions. Derrick's scaling theorem [8] provides further restrictions on solutions. It implies the nonexistence of static solutions in the CP^N model. In order to avoid it, an explicit time dependence can be introduced through the Q-ball ansatz, where one assumes that the phases of all complex fields rotate with equal frequencies ω. Such Q-ball configurations are given by scalar fields proportional to the factor $e^{i\omega t}$; see [9–11].

Some field-theoretic models with standard quadratic kinetic terms possess Q-ball solutions; however, the existence of such solutions requires the inclusion of a potential term into the Lagrangian. The form of the potential in the vicinity of its minimum determines the leading behavior of the scalar field near the vacuum solution. It has been shown in Refs. [12–14] that there is a class of Q-ball solutions which approach the vacuum solution in a quadratic manner; however, it requires a potential with nonvanishing left- and right-hand side derivatives at the minimum. In other words, such a potential is sharp at the minimum (V-shaped potentials) [15]. The models with V-shaped potentials lead to equations of motion containing certain discontinuous terms. A typical field-theoretic model with this property is the signum-Gordon model [12,13,16]. Solutions of such differential equations have a precise mathematical meaning within the formalism of generalized functions. They are so-called *weak solutions* of differential equations [17]. Another very characteristic property of models with V-shaped potentials is the existence of *compactons*, i.e., (solitonic) solutions that differ from a vacuum value on a finite subspace of the base space. In other words, they approach the vacuum at a finite distance and do not have infinitely extended tails—typical for better-known solitons. In spite of the unusual properties of compactons, they find many applications: from condensed matter physics [18] to nuclear physics [19] and cosmology [20]. In fact, the Q-balls presented in Refs. [12–14] are examples of compactons. A distinct approach to compact Q-balls based on potentials containing fractional powers is presented in Ref. [21].

In this paper, we shall construct some finite energy compact solutions of the CP^N model with a V-shaped potential. We are interested in solutions in three spatial dimensions. This work is motivated by an observation that the vortex solutions in models with the CP^N target space defined in $3+1$ dimensions have infinite total energy due to the infinite length of the vortices (energy per unit of length is finite). As we are interested in solutions with finite total energy, the compact Q-balls are very good candidates. First, the Q-ball ansatz allows for time-dependent fields. Second, the compactness of solutions guarantees that the total energy is given by the integral over a finite spatial region. In such a case, there is no problem with the convergence of the integral at spatial infinity. Construction of such solutions in the CP^N model is an important step in searching for similar solutions in effective models like the extended CP^N SF model.

The paper is organized as follows. In Sec. II, we introduce the model and its parametrization. Section III is devoted to the study of compact Q-balls and Q-shells which differ by the number of scalar fields. We compute the Noether charges for such solutions and study how the energy depends on these charges. In Sec. IV, we present an analytic insight into solutions with a small amplitude (the signum-Gordon limit). We obtain exact solutions for the limit model and compare them with numerical solutions of the complete nonlinear model. In the last section, we give some final conclusions.

II. THE MODEL

We shall study a $3+1$-dimensional model with the CP^N target space. The CP^N space is a symmetric space [22], and it can be written as a coset space $CP^N = SU(N+1)/SU(N)\otimes U(1)$ with the subgroup $SU(N)\otimes U(1)$ being invariant under the involutive automorphism ($\sigma^2=1$). The CP^N space has a nice parametrization in terms of the principal variable X (see [23,24]), defined as

$$X(g) \coloneqq g\sigma(g)^{-1}, \qquad g\in SU(N+1). \tag{1}$$

It satisfies $X(gk)=X(g)$ for $\sigma(k)=k$, where $k\in SU(N)\otimes U(1)$. A parametrization of the CP^N model in terms of the variable X is presented in Ref. [25] and of the extended SF model in Ref. [4]. The model we consider here is just the CP^N model extended by a potential (nonderivative) term. As we show below, such a term is crucial to have compactons. The model is given by the Lagrangian

$$\mathcal{L} = -\frac{M^2}{2}\mathrm{Tr}(X^{-1}\partial_\mu X)^2 - \mu^2 V(X), \tag{2}$$

where M has the dimension of mass and the potential $V(X)$ shall be specified in a further part of the paper. It has been pointed out in Ref. [26] that a term proportional to M^2 is just a Lagrangian of the CP^N model. Note that the parametrization of the CP^N model in terms of the principal variable is as good as that in terms of the complex vector $\mathcal{Z}$ defined in the introduction. The reason why we employ the principal variable X instead of $\mathcal{Z}$ is that the extended CP^N SF model [4] has been defined in terms of this variable. In such an approach, a further inclusion of quartic terms (with the intention to search for compact Q-balls in the extended CP^N SF model) would be much easier.

We assume the $(N+1)$-dimensional defining representation in which the $SU(N+1)$ valued group element g is parametrized by the set of complex fields u_i:

$$g \equiv \frac{1}{\vartheta}\begin{pmatrix} \Delta & iu \\ iu^\dagger & 1 \end{pmatrix}, \qquad \Delta_{ij} \equiv \vartheta\delta_{ij} - \frac{u_i u_j^*}{1+\vartheta},$$
$$\vartheta \equiv \sqrt{1+u^\dagger\cdot u}, \tag{3}$$

which leads to the following form of the principal variable (1):

$$X(g) = g^2 = \begin{pmatrix} \mathbb{1}_{N\times N} & 0 \\ 0 & -1 \end{pmatrix} + \frac{2}{\vartheta^2}\begin{pmatrix} -u\otimes u^\dagger & iu \\ iu^\dagger & 1 \end{pmatrix}.$$

The Lagrangian (2) simplifies to the form

$$\mathcal{L} = -M^2\eta^{\mu\nu}\tau_{\nu\mu} - \mu^2 V, \tag{4}$$

where $\eta^{\mu\nu} = \mathrm{diag}(1,-1,-1,-1)$ and

$$\tau_{\nu\mu} \coloneqq -4\frac{\partial_\mu u^\dagger\cdot\Delta^2\cdot\partial_\nu u}{(1+u^\dagger\cdot u)^2}, \quad \text{where } \Delta^2_{ij} = \vartheta^2\delta_{ij} - u_i u_j^*. \tag{5}$$

Variation of the Lagrangian with respect to fields u_i^* leads to a set of equations of motion. All terms containing second derivatives can be uncoupled with the help of the inverse of Δ^2_{ij}, which has the form $\Delta^{-2}_{ij} = \frac{1}{1+u^\dagger\cdot u}(\delta_{ij} + u_i u_j^*)$. It gives

$$\partial_\mu\partial^\mu u_i - 2\frac{(u^\dagger\cdot\partial^\mu u)\partial_\mu u_i}{1+u^\dagger\cdot u} + \frac{\mu^2}{4M^2}(1+u^\dagger\cdot u)\sum_{k=1}^{N}\left[(\delta_{ik}+u_i u_k^*)\frac{\delta V}{\delta u_k^*}\right] = 0. \qquad (6)$$

In order to construct compacton solitons, we have to carefully chose the potential. We know from previous investigations [15,27] that for theories with the usual kinetic term (first derivatives squared) one needs a potential which possesses a linear approach to the vacuum. For example, we may use the following potential:

$$V(X) = \frac{1}{2}[\mathrm{Tr}(\mathbb{1}-X)]^{\frac{1}{2}} = \left(\frac{u^\dagger\cdot u}{1+u^\dagger\cdot u}\right)^{\frac{1}{2}}, \qquad (7)$$

which is the CP^N generalization of the CP^1 (or baby-Skyrme) case [28]. The potential vanishes at $u_i = 0$, i.e., $X = \mathbb{1}$. In the absence of the Skyrme term, the model discussed in Ref. [28] became a $2+1$-dimensional CP^1 model with a potential. The model defined by (2) and (7) is a $3+1$-dimensional model with a V-shaped potential. As has been already announced in the introduction, among the remarkable properties of such models there is a nonvanishing of the first derivative of the potential at the minimum and the existence of compactons. Such compact solutions consist of appropriately matched nontrivial *partial solutions* and a constant vacuum solution. By partial solutions, we mean solutions which hold only on some compact support. Matching surfaces correspond with borders of compactons. Unlike for differentiable potentials, the constant vacuum solution does not satisfy an equation with a nontrivial potential V but rather an equation in the model without potential. The existence of constant solutions can be deduced from the form of the energy density.

In particular, such solutions are almost straightforward in the field-theoretic models which possess a mechanical realization. For instance, in the case of the signum-Gordon model with a single real scalar field, the potential has the form $V \propto |\phi|$, so for $V \neq 0$ the equation of motion is of the form $\partial_\mu\partial^\mu\phi \pm 1 = 0$. Such a model is physically sound, because it can be obtained as a continuous limit of a given mechanical system [15]. Moreover, it became clear from its mechanical realization that $\phi = 0$ is a physical configuration that minimizes the energy (vacuum solution). The vacuum solutions obeys the equation $\partial_\mu\partial^\mu\phi = 0$, and it can be formally included via replacement of the original equation of motion by $\partial_\mu\partial^\mu\phi + \mathrm{sgn}(\phi) = 0$, where $\mathrm{sgn}(0) \coloneqq 0$.

In the model considered in this paper, the energy density is given by the expression

$$\mathcal{H} \coloneqq \frac{\delta\mathcal{L}}{\delta(\partial_0 u_i)}\partial_0 u_i + \frac{\delta\mathcal{L}}{\delta(\partial_0 u_i^*)}\partial_0 u_i^* - \mathcal{L} = -M^2\left(\tau_{00} + \sum_{a=1}^{3}\tau_{aa}\right) + \mu^2 V, \qquad (8)$$

where the index a labels spatial Cartesian coordinates x^a. It vanishes for constant field configurations $u_i = 0$, where $i = 1, \ldots, N$. The vacuum configuration satisfies the homogeneous CP^N equation

$$\partial_\mu\partial^\mu u_i - 2\frac{(u^\dagger\cdot\partial^\mu u)\partial_\mu u_i}{1+u^\dagger\cdot u} = 0, \qquad (9)$$

whereas a nonconstant partial solution must satisfy the equation following from (6):

$$\partial_\mu\partial^\mu u_i - 2\frac{(u^\dagger\cdot\partial^\mu u)\partial_\mu u_i}{1+u^\dagger\cdot u} + \frac{\mu^2}{8M^2}\frac{u_i}{\sqrt{u^\dagger\cdot u}}\sqrt{1+u^\dagger\cdot u} = 0. \qquad (10)$$

The parametrization (3) fixes the global $U(N+1)$ symmetry of the model to $SU(N)\otimes U(1)$. Its subgroup $U(1)^N$ is given by a set of transformations

$$u_i \to e^{i\alpha_i}u_i, \quad i = 1, 2, \ldots, N, \qquad (11)$$

where α_i are some global continuous parameters. Symmetry transformation (11) of the model leads to conserved Noether currents:

$$J^{(i)}_\mu = -\frac{4iM^2}{(1+u^\dagger\cdot u)^2}\sum_{j=1}^{N}[u_i^*\Delta^2_{ij}\partial_\mu u_j - \partial_\mu u_j^*\Delta^2_{ji}u_i]. \qquad (12)$$

Noether currents (12) satisfy the continuity equation $\partial^\mu J^{(i)}_\mu = 0$. If spatial components of currents (12) vanish at spatial infinity, then the integration of this equation on the region of spacetime $[t', t''] \times \mathbb{R}^3$ leads to conserved charges

$$Q^{(i)}_0 = \int_{\mathbb{R}^3} d^3 J^{(i)}_0. \qquad (13)$$

The charges (13) are fundamental quantities in the analysis of the stability of nontopological solutions. They constitute the set of additive conserved quantities. If there is known a relation between the energy of solutions and the Noether charges, then one can evaluate whether splitting the solution into smaller pieces is energetically favorable or not.

III. NONTOPOLOGICAL SOLUTIONS OF THE CP^{2l+1}-TYPE MODEL

We shall restrict our consideration to the case of odd N. The spherical harmonics form the finite representation of eigenfunctions of the angular part of Laplace's operator. In such a case, each complex field can be chosen as proportional to one of $N = 2l + 1$ spherical harmonics labeled by $l = 0, 1, \ldots$. In the present paper, we shall deal with the CP^{2l+1} target space. For further convenience, we shall label the set of $2l + 1$ complex fields by $u_{-l}, \ldots, u_l$ instead of $u_1, u_2, \ldots, u_{2l+1}$.

It is convenient to parametrize the model in terms of dimensionless coordinates. They can be defined in the following way: $\tilde{x}^\mu \coloneqq r_0^{-1} x^\mu$, where r_0 is a constant parameter with the dimension of length. Such a constant can be chosen as the inverse of the dimensional coupling constant M, i.e., $r_0 \equiv M^{-1}$. We consider the ansatz

$$u_m(t, r, \theta, \phi) = \sqrt{\frac{4\pi}{2l+1}} f(r) Y_{lm}(\theta, \phi) e^{i\omega t}, \quad (14)$$

where all coordinates (t, r, θ, ϕ) are dimensionless. They are defined in the following way:

$$\tilde{x}^0 = t, \qquad \tilde{x}^1 = r \sin\theta \cos\phi,$$
$$\tilde{x}^2 = r \sin\theta \sin\phi, \qquad \tilde{x}^3 = r \cos\theta. \quad (15)$$

The integer number l is fixed for a given CP^{2l+1} model, whereas the index m takes values $-l \le m \le l$. Taking into account that $\sum_{m=-l}^{l} Y_{lm}^*(\theta, \phi) Y_{lm}(\theta, \phi) = \frac{2l+1}{4\pi}$, we include the factor $\sqrt{\frac{4\pi}{2l+1}}$ in (14) to simplify the formulas. It follows that $u^\dagger \cdot u = f^2(r)$ depends only on the radial coordinate r. Similarly, many other terms either vanish or depend only on the radial coordinate; see the Appendix. The field equations (9) and (10) result in a single ordinary differential equation:

$$f'' + \frac{2}{r} f' + \omega^2 \frac{1 - f^2}{1 + f^2} f - \frac{l(l+1)}{r^2} f - \frac{2 f f'^2}{1 + f^2} = \frac{\tilde{\mu}^2}{8} \mathrm{sgn}(f) \sqrt{1 + f^2}, \quad (16)$$

where $\tilde{\mu}^2 \coloneqq \mu^2 / M^4$ and where we have adopted the definition of the sgn() function such that $\mathrm{sgn}(f) \coloneqq 1$ for $f > 0$ and $\mathrm{sgn}(0) \coloneqq 0$. This is the main equation we will further analyze in the paper.

The Hamiltonian density (8) can be written as $\mathcal{H} = M^4 H$, where H is a dimensionless expression:

$$H = -\left[\tau_{tt} + \tau_{rr} + \frac{1}{r^2}\left(\tau_{\theta\theta} + \frac{1}{\sin^2\theta} \tau_{\phi\phi}\right)\right] + \tilde{\mu}^2 V.$$

For the class of solutions given by (14), we get a dimensionless energy density which is a function of the radial coordinate itself:

$$H = \frac{4}{(1 + f^2)^2}\left[f'^2 + \left(\omega^2 + \frac{l(l+1)}{r^2}(1 + f^2)\right) f^2\right] + \tilde{\mu}^2 \sqrt{\frac{f^2}{1 + f^2}}. \quad (17)$$

A total dimensionless energy is given by the integral

$$E = \int_{\mathbb{R}^3} d\Omega dr r^2 H = 4\pi \int_0^\infty dr r^2 H. \quad (18)$$

Let us consider the Noether currents (12). Since in dimensionless Cartesian coordinates $\tilde{x}^\mu$ the partial derivatives are of the form $\frac{\partial}{\partial x^\mu} = M \frac{\partial}{\partial \tilde{x}^\mu}$, one can define expressions $\tilde{J}_\mu^{(m)}$ as dimensionless quantities $J_\mu^{(m)} = M^3 \tilde{J}_\mu^{(m)}$, where the index $i = 1, \ldots, 2l + 1$ has been replaced by the index $m = -l, \ldots, l$. The complex fields u_m are functions of the curvilinear dimensionless coordinates $\xi^\mu \to \{t, r, \theta, \phi\}$. The Noether currents written in dependence of these coordinates, i.e., $\tilde{J}_\mu^{(m)}(\xi)$, must satisfy the continuity equation

$$\frac{1}{\sqrt{-g}} \partial_\mu (\sqrt{-g} g^{\mu\nu} \tilde{J}_\nu^{(m)}(\xi)) = 0,$$

where $g^{\mu\nu} = \mathrm{diag}(1, -1, -\frac{1}{r^2}, -\frac{1}{r^2 \sin^2\theta})$ and $\sqrt{-g} = r^2 \sin\theta$. It turns out that there are only two nonvanishing components of the Noether currents, namely,

$$\tilde{J}_t^{(m)}(r, \theta) = 8\omega \frac{(l-m)!}{(l+m)!} \frac{f^2}{(1 + f^2)^2} (P_l^m(\cos\theta))^2, \quad (19)$$

$$\tilde{J}_\phi^{(m)}(r, \theta) = 8m \frac{(l-m)!}{(l+m)!} \frac{f^2}{1 + f^2} (P_l^m(\cos\theta))^2. \quad (20)$$

Note that both nonvanishing components depend neither on t nor ϕ. It follows that the continuity equation $\partial_t J_t^{(m)} + \frac{1}{r^2 \sin^2\theta} \partial_\phi J_\phi^{(m)} = 0$ is satisfied explicitly. The Noether charges can be obtained by integrating the continuity equation in the region $[t', t''] \times \mathbb{R}^3$:

$$\int_{t'}^{t''} dt \int_{\mathbb{R}^3} d^3\xi [\sqrt{-g} \partial_t \tilde{J}_t^{(m)} + \partial_a (\sqrt{-g} g^{ab} \tilde{J}_b^{(m)})] = 0, \quad (21)$$

where $a, b = \{1, 2, 3\}$. The second term can be written as a surface integral at spatial infinity, and it gives no contribution to the integral if $\tilde{J}_b^{(m)}$ vanish sufficiently quickly at spatial infinity. The remaining term expresses equality of the Noether charges:

$$Q_t^{(m)} \coloneqq \frac{1}{2}\int_{\mathbb{R}^3} d^3\xi\sqrt{-g}\tilde{J}_t^{(m)}(\xi) \qquad (22)$$

at t' and t''. The factor $\frac{1}{2}$ has been introduced for further convenience. Plugging (19) into (22), we get

$$Q_t^{(m)} = \omega\frac{16\pi}{2l+1}\int_0^\infty drr^2\frac{f^2}{(1+f^2)^2}. \qquad (23)$$

All the Noether charges have the same value, because (23) does not depend on m. Notice that the contribution to the total energy which has an origin in τ_{tt} (proportional to ω^2) can be expressed in terms of the Noether charges as a sum $\sum_{m=-l}^{l}\omega Q_t^{(m)}$. In fact, contributions to the energy which have an origin in terms $\tau_{\theta\theta}$ and $\tau_{\phi\phi}$ can also be represented in the form of the sum. We have already seen that spatial components of the Noether currents do not contribute to the charges; however, they are useful to define the integrals

$$Q_\phi^{(m)} \coloneqq \frac{3}{2}\int_{\mathbb{R}^3} d^3\xi\sqrt{-g}\frac{\tilde{J}_\phi^{(m)}(\xi)}{r^2}. \qquad (24)$$

Plugging (20) into (24) and making use of the standard orthogonality relation for the associated Legendre functions $\int_{-1}^{1}dx(P_l^m(x))^2 = \frac{2}{2l+1}\frac{(l+m)!}{(l-m)!}$, we get

$$Q_\phi^{(m)} = m\frac{48\pi}{2l+1}\int_0^\infty dr\frac{f^2}{1+f^2}. \qquad (25)$$

The total energy E can be expressed in terms of the Noether charges $Q_t^{(m)}$ and the integrals $Q_\phi^{(m)}$, and it reads

$$E = 4\pi\int_0^\infty drr^2\left(\frac{4f'^2}{(1+f^2)^2} + \tilde{\mu}^2\sqrt{\frac{f^2}{1+f^2}}\right) + \sum_{m=-l}^{l}(\omega Q_t^{(m)} + mQ_\phi^{(m)}), \qquad (26)$$

where we have made use of the expression $\sum_{m=-l}^{l}m^2 = \frac{1}{3}l(l+1)(2l+1)$. In the subsequent part of the paper, we shall construct some nontopological compact solutions of Eq. (16).

A. Expansion at the center

Plugging the series expansion of $f(r)$ at $r=0$,

$$f(r) = \sum_{k=0}^{\infty}a_k r^k, \qquad (27)$$

into Eq. (16), we get

$$\sum_{k=0}^{\infty}b_k r^{k-2} = 0, \qquad (28)$$

where the lowest three coefficients b_0, b_1, and b_2 have the form, respectively,

$$\begin{aligned} b_0 &= l(l+1)a_0, \\ b_1 &= (l-1)(l+2)a_1, \\ b_2 &= (l-2)(l+3)a_2 \\ &\quad + \frac{\tilde{\mu}^2}{8}\sqrt{1+a_0^2} + \left[\frac{2(a_1^2+a_0^2\omega^2)}{1+a_0^2} - \omega^2\right]a_0. \end{aligned}$$

We have assumed $\mathrm{sgn}(f)=1$, because we are looking for a nontrivial solution. Equation (28) is fulfilled if a_k are such that all coefficients b_k vanish. It turns out that the form of expansion (27) is sensitive to the value of the number l, i.e., the number of complex scalar fields u_m, where $m=-l,\ldots,l$. In the following part, we study some qualitatively different forms of expansion for $l=0$, $l=1$, and $l\geq 2$.

1. Case $l=0$

For $l=0$, Eq. (28) can be satisfied in the leading term of expansion if $a_1=0$. A more detailed study shows that the choice $a_1=0$ implies the vanishing of all odd-order coefficients a_{2j+1}, where $j=1,2,3,\ldots$. Indeed, one can check that if for some fixed odd number n all odd lower-order coefficients vanish $a_1=a_3=\cdots=a_{n-2}=0$ (and consequently vanish all odd-order coefficients up to b_{n-2}), then the next odd-order coefficient b_n is of the form $b_n = a_n(l-n)(l+1+n)$. Consequently, in order to put $b_n=0$, one has to set $a_n=0$. All even coefficients a_{2j} are uniquely determined by a_0, which is a free parameter of the expansion. The lowest-order terms of the expansion of the function $f(r)$, given by (27), read

$$f(r) = a_0 + \left[\frac{\tilde{\mu}^2}{48}\sqrt{1+a_0^2} - \frac{a_0(1-a_0^2\omega^2)}{6(1+a_0^2)}\right]r^2 + \mathcal{O}(r^4). \qquad (29)$$

A value of the coefficient a_0 can be determined only for a complete solution that must be regular at the center and at the boundary. A numerical analysis shows that a physically relevant solution must have $a_2<0$; otherwise, the solution grows up infinitely with r. The coefficient a_2 depends on the parameter ω. It turns out that there is a lower bound for ω. The region $a_2<0$ has been sketched in Fig. 1. It suggest the existence of a minimal value of ω_m for which there still exists a compact solution with finite energy. Note that the border of the region plotted in Fig. 1 does not determine a value ω_m, but it rather constitutes its limitation. The value of ω_m can be obtained by performing a numerical

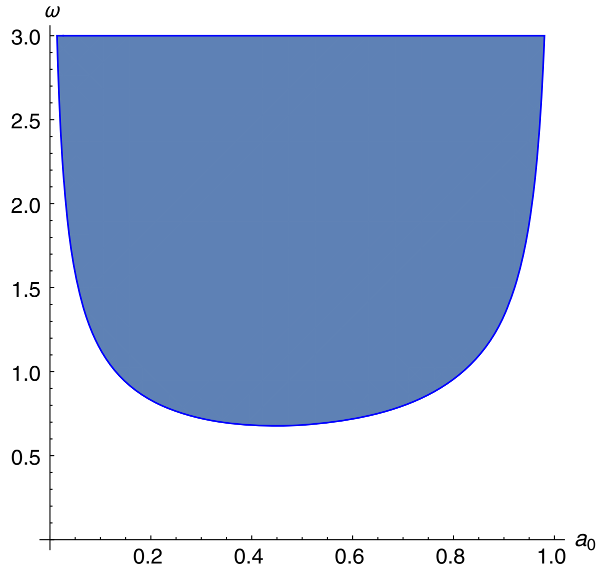

FIG. 1. The region $a_2 < 0$ in dependence on a_0 and ω for the case of $l = 0$, where in addition we set $\tilde{\mu} = 1$.

integration of the radial equation (16). It follows from the expansion of (17) at $r = 0$,

$$H(r) = a_0\left[\frac{\tilde{\mu}^2}{\sqrt{1+a_0^2}} + \frac{4a_0\omega^2}{(1+a_0^2)^2}\right] + \mathcal{O}(r^2), \quad (30)$$

that the energy density for $l = 0$ does not vanish at the center of the Q-ball.

2. Case l = 1

For $l = 1$, the coefficient a_1 became a free parameter, whereas a_0 must vanish. The coefficient a_2 is determined by the strength coupling constant $\tilde{\mu}^2$. Except a_2, all higher-order coefficients a_k contain a_1. The next three coefficients of the expansion read

$$a_2 = \frac{\tilde{\mu}^2}{32}, \quad a_3 = \frac{a_1}{10}(2a_1 - \omega^2), \quad a_4 = \frac{\tilde{\mu}^2}{576}(12a_1^2 - \omega^2). \quad (31)$$

Although the radial function satisfies $f(r = 0) = 0$, the energy density is still nonzero at the center. It can be seen from

$$H(r) = 12a_1^2 + 2\tilde{\mu}^2 a_1 r + \left[\frac{7}{128}\tilde{\mu}^4 - 8a_1^4\right] r^2 + \mathcal{O}(r^3). \quad (32)$$

3. Case l ≥ 2

It follows from the expansion (28) that for $l = 2, 3, \ldots$ both coefficients a_0 and a_1 must vanish. Taking $a_0 = a_1 = 0$, we get $b_2 = \frac{\tilde{\mu}^2}{8}$, so the radial equation is not satisfied. It follows that there is no nonvanishing solution in the vicinity of $r = 0$. However, it does not mean that there is no solution at all. The radial function cannot be nontrivial at the center, but it can be nontrivial at some region $r \in (R_1, R_2)$. Outside this region, i.e., at $r \in [0, R_1]$ and at $r \in [R_2, \infty)$, the function $f(r)$ must vanish identically. A vacuum solution in the vicinity of $r = 0$ corresponds with $\mathrm{sgn}(f) = 0$ in (16). A term in b_2 containing $\tilde{\mu}^2$ is in fact proportional to $\mathrm{sgn}(f)$, so it became absent now. In such a case, the solution has the form of a compact spherical shell. The discussion of the behavior of the radial function $f(r)$ at the inner R_1 and the outer R_2 radius is essentially the same. It is the subject of the next paragraph.

B. Expansion at the boundary

As we consider compact solutions, the vacuum solution $f(r) = 0$ holds for $r > R$, which leads to the vanishing of the energy density in this region. A symbol R stands for the compacton radius in the case $l = 0$, 1 and the outer compacton radius $R \equiv R_2$ for $l = 2, 3, \ldots$. The continuity of the energy density imposes conditions on the leading behavior of the solution in the region $r \leq R$. Such a solution must satisfy the following conditions at the border:

$$f(R) = 0, \qquad f'(R) = 0. \quad (33)$$

Plugging the expression $f(r) = A(R - r)^\alpha + \cdots$ into (16), one can find

$$-A\alpha(\alpha - 1)(R - r)^{\alpha-2} + \frac{\tilde{\mu}^2}{8} + \cdots = 0. \quad (34)$$

The leading term of (34) vanishes for $\alpha = 2$ and an appropriate value of A. It suggests that solutions possess a quadratic leading behavior at the border:

$$f(r) = \sum_{k=2}^{\infty} A_k (R - r)^k. \quad (35)$$

It turns out that all coefficients A_k are determined in terms of the compacton radius R and parameters of the model. The lowest three coefficients read

$$A_2 = \frac{\tilde{\mu}^2}{16}, \qquad A_3 = \frac{\tilde{\mu}^2}{24R},$$
$$A_4 = \frac{\tilde{\mu}^2}{192R^2}[l(l+1) + 8 - R^2\omega^2]. \quad (36)$$

It leads to the following expansion of the energy density at the compacton boundary:

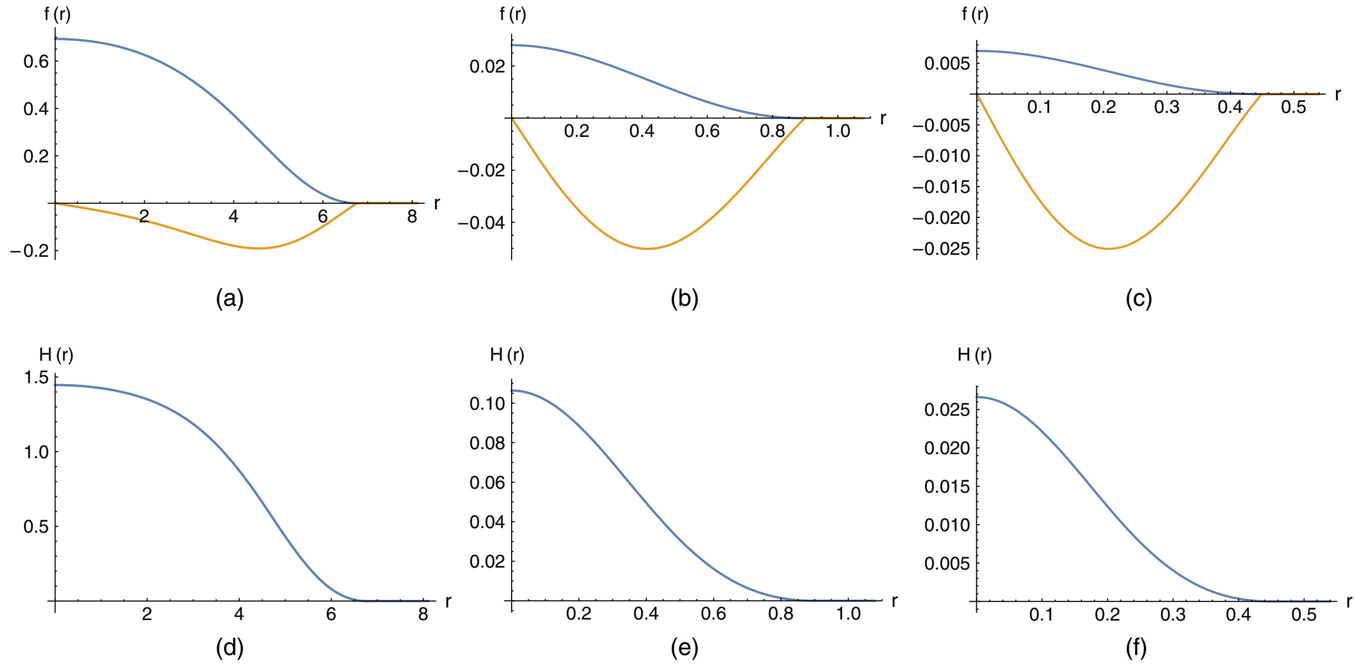

FIG. 2. The radial function $f(r)$ (upper curve), its derivative $f'(r)$ (bottom curve), and the energy density $H(r)$ for $l = 0$ and (a),(d) $\omega = 1.0$, (b), (e) $\omega = 5.0$, and (c),(f) $\omega = 10.0$.

$$H(r) = \frac{\tilde{\mu}^2}{8}(R-r)^2 + \frac{\tilde{\mu}^4}{6R}(R-r)^3 + \frac{\tilde{\mu}^4}{96R^2}[4l(l+1) + 26 - R^2\omega^2](R-r)^4 + \cdots. \quad (37)$$

The lowest-order terms do not depend on the integer number l; i.e., they have the same form independently of the number of complex scalar fields. The first term which depends on l is proportional to $(R-r)^4$.

For the case $l \geq 2$, i.e., when the solution has the form of a shell-shaped compacton, the radial function possesses expansion $f(r) = B_2(r - R_1)^2 + \cdots$ at the inner compacton radius R_1. The expansion coefficients are almost the same as for the outer compacton radius, and they read $B_k = (-1)^k A_k$.

C. Numerical solutions

We adopt a shooting method for the numerical integration of the radial equation (16). We impose the initial conditions for numerical integration in the form of the first few terms of a series expansion at $r = 0$ for $l = 0$, 1 or $r = R$ for $l \geq 2$. In the numerical computation, we substitute $r = 0$ by $r = \varepsilon = 10^{-4}$. There is only one free parameter which determines the expansion series at the center, namely, a_0 for $l = 0$ and a_1 for $l = 1$. On the other hand, a series expansion at the boundary has also one free parameter, which is the compacton radius R. There is exactly one curve being a solution of the second-order ordinary differential equation which simultaneously satisfies conditions at the center and at the boundary. For a chosen value of a_0 or a_1, we integrate numerically the radial equation and determine a value of the radius $\bar{R}$ such that $f'(\bar{R}) = 0$. A value of the expression $f(\bar{R})$ is used to modify an initial shooting parameter according to $f(\bar{R}) \to 0$ for $\bar{R} \to R$. The loop is interrupted when $|f(\bar{R})| < 10^{-6}$. The examples of numerical solutions for $l = 0$ and different values of the parameter ω are presented in Fig. 2. The compacton profile functions $f(r)$ and their first derivatives $f'(r)$ are sketched in Figs. 2(a)–2(c). The respective energy densities are presented in Figs. 2(d)–2(f). The energy density has a maximum at the center $r = 0$.

The profile functions $f(r)$ and the energy density plots are shown in Fig. 3. The fundamental difference between the cases $l = 1$ and $l = 0$ case is a form of the solution at $r = 0$. For $l = 1$ the function $f(r)$ vanishes at the center, whereas its first derivative $f'(r = 0)$ is finite. The energy density does not vanish at the center $r = 0$; however, $H(0)$ is not a maximal value anymore. The maximum of $H(r)$ is reached at some finite distance from the center.

The shooting parameter for $l \geq 2$ can be chosen as one of the compacton radii R_1 and R_2. We fine-tune a smaller radius R_1 in order to minimize the solution at the larger radius $f(\bar{R}) \to 0$ for $\bar{R} \to R_2$, where $\bar{R}$ is a solution of the equation $f'(\bar{R}) = 0$. We interrupt the loop when accuracy 10^{-6} is reached. The function $f(r)$ is bell-shaped, so each u_m is nontrivial in the region given by a spherical shell limited by the internal R_1 and the external R_2 radius. The numerical values of the compacton radii grow with the

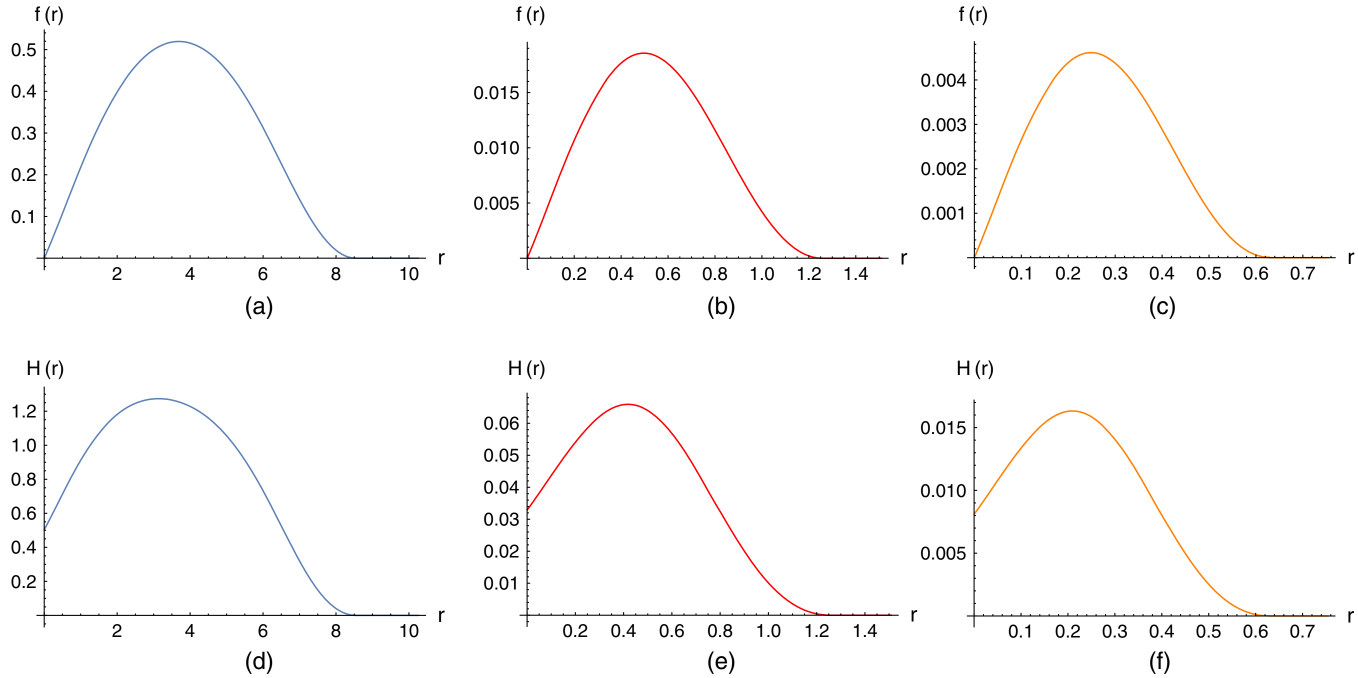

FIG. 3. The radial function $f(r)$ and the energy density $H(r)$ for $l = 1$ and (a),(d) $\omega = 1.0$, (b), (e) $\omega = 5.0$, and (c), (f) $\omega = 10.0$.

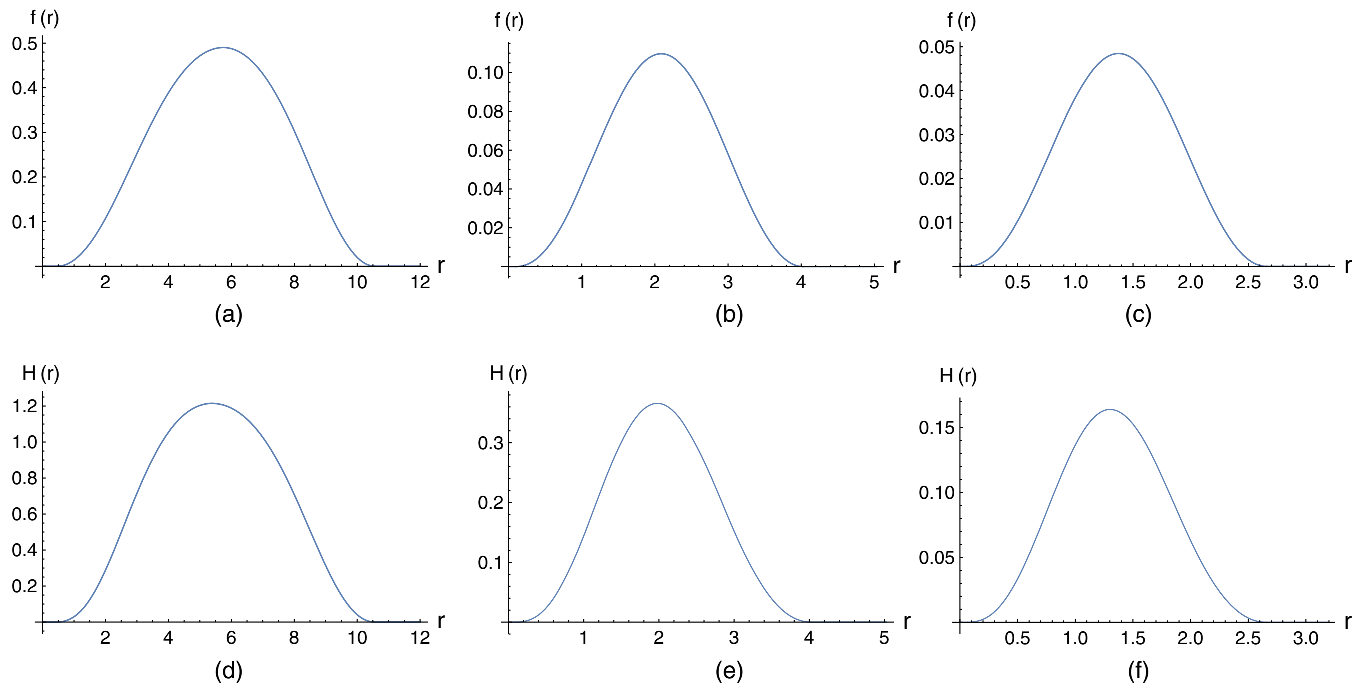

FIG. 4. The radial function $f(r)$ and the energy density $H(r)$ for $l = 2$ and (a), (d) $\omega = 1.0$, (b), (e) $\omega = 2.0$, and (c), (f) $\omega = 3.0$.

model parameter l. It can be easily seen by comparing Figs. 4 and 5. The compacton radii ($l \geq 2$) are decreasing functions of the parameter ω. A very similar behavior can be observed for $l = 0, 1$. In Fig. 6, we plot the compacton size $\delta R \coloneqq R_2 - R_1$ in dependence on the parameter ω. Clearly, $R_1 \equiv 0$ for $l = 0, 1$. For better transparency, we plot a function $(\delta R)^{-1}(\omega)$. The function $(\delta R)^{-1}$ has linear asymptotic behavior for $\omega \gg 1$. For small values of the parameter ω, the function $(\delta R)^{-1}(\omega)$ is not a linear function any longer; see Fig. 6(a). One of the simplest functions

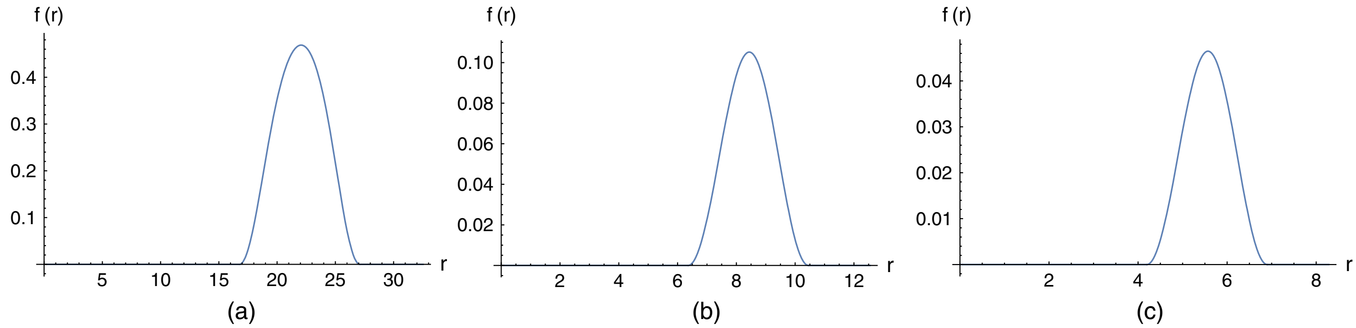

FIG. 5. The radial function $f(r)$ for $l = 10$ and (a) $\omega = 1.0$, (b) $\omega = 2.0$, and (c) $\omega = 3.0$.

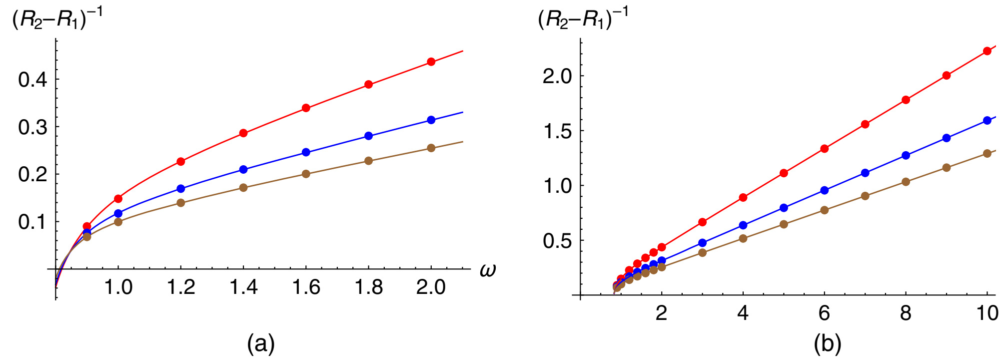

FIG. 6. The inverse of the compacton size $\delta R \coloneqq R_2 - R_1$ in dependence on ω for (from top to bottom) $l = 0$, $l = 1$, and $l = 2$. The inner radius is $R_1 \equiv 0$ for $l = 0$ and $l = 1$.

that can be fitted to the numerical data is a rational function

$$(\delta R)^{-1}(\omega) = \frac{a\omega^2 + b\omega + c}{d\omega + e}. \tag{38}$$

The fit coefficients are presented in Table I.

Expression (38) has the following asymptotic form for $\omega \to \infty$:

$$(\delta R)^{-1}(\omega) = \frac{a}{d}\omega + \frac{bd - ae}{d^2} + \mathcal{O}(\omega^{-1}). \tag{39}$$

We define the coefficients $A_1 \coloneqq \frac{a}{d}$ and $B_1 \coloneqq \frac{bd-ae}{d^2}$. Their numerical values are presented in Table II.

A very similar analysis can be performed for the dimensionless energy of the compacton. We observe that the expression $E^{-1/5}$ is a linear function of ω for $\omega \gg 1$. The plot of this function is shown in Fig. 7, where the deviation from linear behavior is observed for small values of ω. The curves that represent the fits are given by rational functions $E^{-1/5}(\omega) = (\tilde{a}\omega^2 + \tilde{b}\omega + \tilde{c})/(\tilde{d}\omega + \tilde{e})$. We shall not present the numerical values of coefficients; instead, we give in Table II the list of coefficients of the asymptotic expression $E^{-1/5} = A_2\omega + B_2$ for $\tilde{\mu} = 1, \omega \gg 1$.

Another important point is an analysis of the Noether charges and their relation to the energy of the solution. The plot of these charges is presented in Fig. 8(a). We observe that for $\omega \gg 1$ the charges behave as $Q_t \propto \omega^{-6}$. We shall omit the index m, because the Noether charges do not depend on it. In Fig. 8(b), we plot relation energy charge for some Q-balls $l = 0, 1$ and some Q-shells $l = 2$. The leading behavior of the function $Q_t^{-1/6}$ in the limit $\omega \gg 1$ is given by $Q_t^{-1/6} = A_3\omega + B_3$. Numerical values of the coefficients A_3 and B_3 are presented in Table III. We also present the coefficients A_4 and B_4, which are related to

TABLE I. The fit coefficients of (38).

	a	b	c	d	e
$l = 0$	2223.78	−1388.73	−357.34	10044.60	−6859.62
$l = 1$	53.86	−36.61	53.86	39.62	−244.81
$l = 2$	169.46	−118.27	−15.73	1316.28	−960.93

TABLE II. Coefficients of oblique asymptotes $\delta R^{-1} = A_1\omega + B_1$ and $E^{-1/5} = A_2\omega + B_2$.

	A_1	B_1	A_2	B_2
$l = 0$	0.221	0.012	0.369	0.014
$l = 1$	0.158	0.006	0.287	0.004
$l = 2$	0.128	0.004	0.243	0.005

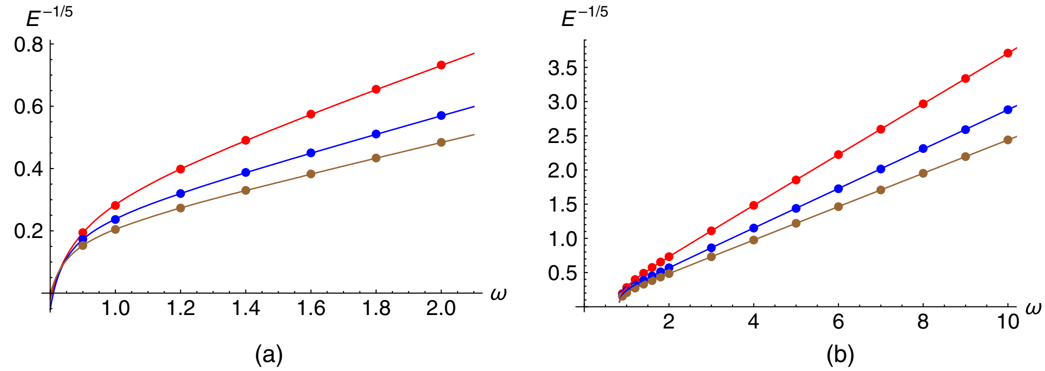

FIG. 7. The compacton energy function in dependence on ω for (from top to bottom) $l = 0$, $l = 1$, and $l = 2$.

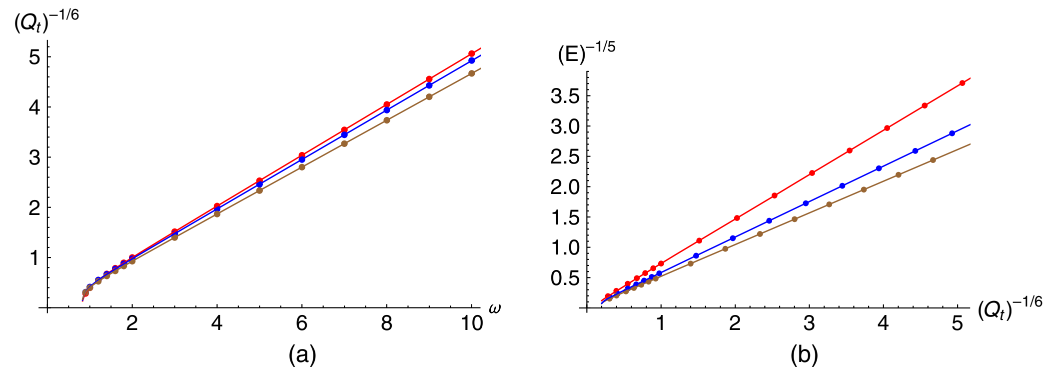

FIG. 8. (a) Noether charge Q_t for (from top to bottom) $l = 0$, $l = 1$, and $l = 2$ in dependence on ω. (b) A relation between Noether charges and the energy of the solution for (from top to bottom) $l = 0$, $l = 1$, and $l = 2$.

the expression $E^{-1/5} = A_4 Q_t^{-1/6} + B_4$. One can conclude from Fig. 8(b) that the relation between the energy $E^{-1/5}$ and the Noether charges $Q_t^{-1/6}$ is linear with a very good accuracy, even though in the region of small ω. It means that the energy of compactons behaves as $E \propto Q_t^{\frac{5}{6}}$ in the whole range of ω. The value of the power suggests that the splitting of a single Q-ball solution into two Q-balls is not energetically favorable, because $E(Q_1 + Q_2) < E(Q_1) + E(Q_2)$. This argument is usually presented in the discussion of the stability of Q-ball solutions [12].

Finally, we plot the medium radius of some compact shells $R_0 \coloneqq \frac{1}{2}(R_1 + R_2)$ in dependence on l. Figure 9(a) shows R_0 for $l = 2, 3, \ldots, 10$ and for three different values of $\omega = 1.0$, $\omega = 2.0$, and $\omega = 3.0$. The medium radius of compactons grows linearly with l. A linear fit gives $R_0 \approx 1.31 + 2.06l$ for $\omega = 1.0$, $R_0 \approx 0.44 + 0.79l$ for $\omega = 2.0$, and $R_0 \approx 0.29 + 0.52l$ for $\omega = 3.0$. The medium radius R_0 decreases as ω grows.

In Fig. 9(b), we show the square root of the energy of compactons in dependence on l. The linear fits are given by $\sqrt{E} \approx 15.13 + 18.38l$ for $\omega = 1.0$, $\sqrt{E} \approx 1.59 + 2.23l$ for $\omega = 2.0$, and $\sqrt{E} \approx 0.56 + 0.80l$ for $\omega = 3.0$. Note that linear regression is useful for the extrapolation of the functions $R_0(l)$ and $\sqrt{E(l)}$ to higher integers l, whereas interpolation to noninteger values is meaningless.

TABLE III. Coefficients of oblique asymptotes $Q_t^{-1/6} = A_3\omega + B_3$ and $E^{-1/5} = A_4 Q_t^{-1/6} + B_4$.

	A_3	B_3	A_4	B_4
$l = 0$	0.504	0.017	0.731	0.003
$l = 1$	0.491	0.008	0.584	0.001
$l = 2$	0.466	0.009	0.522	0.001

IV. THE SIGNUM-GORDON LIMIT

According to our numerical results, the size of the compactons, their energy, and the Noether charges behave in the limit $\omega \to \infty$ as some powers of ω. In this section, we shall study this problem from an analytic point of view. There are many exact results which can be obtained for a model which is a limit version of the CP^N-type model (4).

A numerical analysis shows that the maximal values of the functions $f(r)$ and $|f'(r)|$ tend to zero as ω increases. Clearly, in this limit the model can be approximated by the complex signum-Gordon–type model with the equation of motion

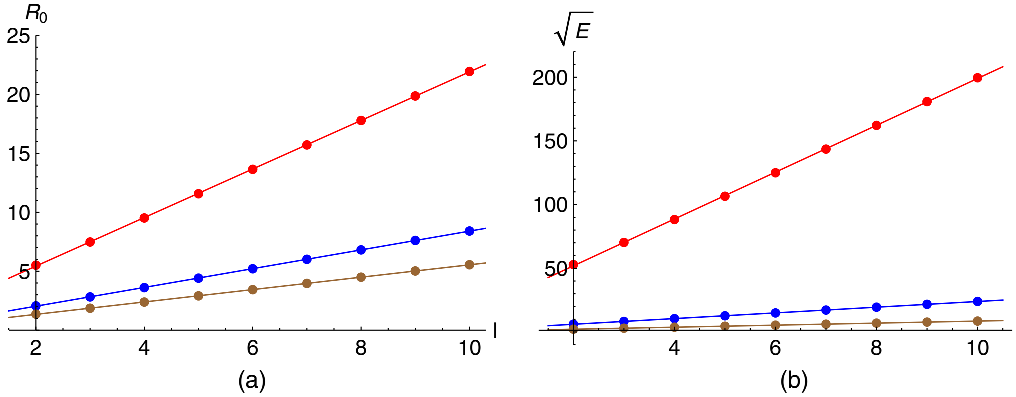

FIG. 9. (a) The medium radius $R_0 = \frac{1}{2}(R_1 + R_2)$ of compact shells in dependence on $l = 2, \ldots, 10$. From top to bottom: $\omega = 1.0$, $\omega = 2.0$, and $\omega = 3.0$. (b) The compacton energy square root in dependence on $l = 2, \ldots, 10$.

$$\partial^2 u_i + \frac{\mu^2}{8M^2} \frac{u_i}{\sqrt{u^\dagger \cdot u}} = 0 \tag{40}$$

for $u_i \neq 0$ and $\partial^2 u_i = 0$ for $u_i = 0$. To be more precise, Eq. (40) is the complex signum-Gordon equation of motion only for $l = 0$, i.e., for the model that possesses exactly one complex field u. For $l \geq 1$, the model is parametrized by $2l + 1$ complex fields coupled via a potential term. For this reason, we call it the signum-Gordon–type model. The solutions of the model described by (40) can be seen as some limit solutions $|u_i| \ll 1$ of the CP^N-type model discussed above. In the further part of this section, we show that the proportionality relations $\delta R \propto \omega^{-1}$ and $E \propto \omega^{-5}$ are exact for the signum-Gordon–type model. Next we shall discuss the relation between the energy and the Noether charges.

The equations of motion (40) for the ansatz (14) is reduced to a single radial equation. In terms of new radial variable $x \coloneqq \omega r$, the radial equation takes the form

$$\tilde{f}''(x) + \frac{1}{x}\tilde{f}'(x) + \left(1 - \frac{l(l+1)}{x^2}\right)\tilde{f}(x) = \alpha^2 \mathrm{sgn}(\tilde{f}(x)), \tag{41}$$

where $\tilde{f}(x) \coloneqq f(\frac{x}{\omega}) \equiv f(r)$, $\tilde{f}'(x) \equiv \frac{d\tilde{f}}{dx}$, $\alpha^2 \coloneqq \frac{\tilde{\mu}^2}{8\omega^2}$, and $\tilde{\mu}^2 \coloneqq \frac{\mu^2}{M^4}$ is a dimensionless coupling constant defined in the same way as for the CP^N-type model. The energy density is given by

$$H = 4\omega^2 \left[\left(\frac{d\tilde{f}}{dx}\right)^2 + \left(1 + \frac{l(l+1)}{x^2}\right)\tilde{f}^2\right] + \tilde{\mu}^2 |\tilde{f}|. \tag{42}$$

Equation (41) is a spherical Bessel equation, nonhomogeneous for $\mathrm{sgn}(\tilde{f}) = 1$ and homogeneous for $\mathrm{sgn}(\tilde{f}) = 0$. The radial equation possesses exact solutions. The compact solutions consist of some nontrivial solutions of the nonhomogeneous equation which are matched with the vacuum solution $\tilde{f} = 0$. In the case $\mathrm{sgn}(\tilde{f}) = 1$, the solution is a sum of a general solution of the homogeneous equation and any particular solution $\tilde{f}_p(x)$ of the nonhomogeneous equation, i.e.,

$$\tilde{f}(x) = \mathcal{A} j_l(x) + \mathcal{B} n_l(x) + \tilde{f}_p(x), \tag{43}$$

where $\mathcal{A}$ and $\mathcal{B}$ are free constants. The spherical Bessel functions $j_l(x)$ and the spherical Neumann functions $n_l(x)$ form linearly independent solutions of the spherical Bessel equation, so their Wronskian is different from zero:

$$W(x) = j_l(x) n_l'(x) - j_l'(x) n_l(x) = \frac{1}{x^2} \neq 0. \tag{44}$$

The particular solution can be determined by the method of variation of parameters; i.e., it is of the form

$$\tilde{f}_p(x) = a(x) j_l(x) + b(x) n_l(x), \tag{45}$$

where $a(x)$ and $b(x)$ must be such that they satisfy the equations $a'(x) j_l(x) + b'(x) n_l(x) = 0$ and $a'(x) j_l'(x) + b'(x) n_l'(x) = \alpha^2$. They have the solutions $a'(x) = -\frac{\alpha^2 n_l(x)}{W(x)}$ and $b'(x) = \frac{\alpha^2 j_l(x)}{W(x)}$, which after integration read

$$a(x) = -\alpha^2 \int dx x^2 n_l(x), \quad b(x) = \alpha^2 \int dx x^2 j_l(x). \tag{46}$$

The particular solutions $\tilde{f}_p(x)$ are given in terms of spherical Bessel functions, the sine integral $\mathrm{Si}(x) \coloneqq \int_0^x dt \frac{\sin t}{t}$, and the cosine integral $\mathrm{Ci}(x) \coloneqq -\int_x^\infty dt \frac{\cos t}{t}$. The first five particular solutions labeled by $l = 0, \ldots, 4$ have the form

$$\tilde{f}_p^{(l=0)}(x) = \alpha^2, \tag{47}$$

$$\tilde{f}_p^{(l=1)}(x) = \alpha^2 \left(1 + \frac{2}{x^2}\right), \tag{48}$$

$$\tilde{f}_p^{(l=2)}(x) = \alpha^2\left(1+\frac{9}{x^2}\right) + 3\alpha^2[\mathrm{Ci}(x)j_2(x) + \mathrm{Si}(x)n_2(x)], \tag{49}$$

$$\tilde{f}_p^{(l=3)}(x) = \alpha^2\left(1+\frac{12}{x^2}+\frac{120}{x^4}\right), \tag{50}$$

$$\tilde{f}_p^{(l=4)}(x) = \alpha^2\left(1+\frac{25}{2x^2}+\frac{1575}{2x^4}\right) + \frac{15\alpha^2}{2}[\mathrm{Ci}(x)j_4(x) + \mathrm{Si}(x)n_4(x)]. \tag{51}$$

A solution with $l = 0$ must take some nonzero value at the center $x = 0$. This condition can be satisfied for $\mathcal{B} = 0$. The remaining free parameters, which are the constant $\mathcal{A}$ and the compacton radius x_R, can be determined from $f(x_R) = 0$ and $f'(x_R) = 0$. It gives $x_R = x_1^1$, where $x_1^1 = 4.49341$ is a first nontrivial zero of the spherical Bessel function $j_1(x)$. The trivial zero is just $x_0^1 = 0$. The profile of the compacton is given by

$$\tilde{f}(x) = \alpha^2\left(1-\frac{j_0(x)}{j_0(x_1^1)}\right). \tag{52}$$

Since $\alpha^2 = \frac{\tilde{\mu}^2}{8\omega^2}$, the radial profile function behaves as $\tilde{f}(x) = f(r) \propto \omega^{-2}$. From the definition of the variable $x = \omega r$, one gets

$$R^{-1} = \frac{\omega}{x_1^1} \approx 0.22254\omega. \tag{53}$$

This formula allows us to interpret the coefficient A_1 for $l = 0$ in Table II as the inverse of the first nontrivial zero of $j_1(x)$.

For the model with $l = 1$, the profile function reaches zero at $x = 0$ and has a nonvanishing first derivative at the center. It gives $\mathcal{B} = 2\alpha^2$ in (43). In order to satisfy the boundary conditions at the compacton border, one has to choose $\mathcal{A} = 2\pi\alpha^2$ and $x_R = 2\pi$. The solution is then of the form

$$\tilde{f}(x) = \alpha^2\left(1+\frac{2}{x^2}+2\pi j_1(x)+2n_1(x)\right), \tag{54}$$

where $j_1(x) = \frac{\sin(x)}{x^2} - \frac{\cos(x)}{x}$ and $n_1(x) = -\frac{\cos(x)}{x^2} - \frac{\sin(x)}{x}$. The profile function is proportional to ω^{-2}, and the compacton radius obeys the relation

$$R^{-1} = \frac{\omega}{2\pi} \approx 0.15915\omega, \tag{55}$$

which allows us to interpret A_1 for $l = 1$ in Table II as $A_1 = \frac{1}{2\pi}$.

Let us consider the model with $l = 2$. The compacton radii x_1 and x_2 where $x_1 < x_2$ are such that $\tilde{f}(x_1) = 0$, $\tilde{f}'(x_1) = 0$ and similarly $\tilde{f}(x_2) = 0$, $\tilde{f}'(x_2) = 0$. The boundary conditions at x_1 allow us to determine the constants $\mathcal{A}$ and $\mathcal{B}$ in (43). The solution takes the form

$$\begin{aligned}\tilde{f}(x) \coloneqq{}& \alpha^2\left(1+\frac{9}{x^2}\right) + \alpha^2(4\cos x_1 + x_1\sin x_1 \\ &+ 3[\mathrm{Ci}(x) - \mathrm{Ci}(x_1)])j_2(x) \\ &+ \alpha^2(4\sin x_1 - x_1\cos x_1 + 3[\mathrm{Si}(x) - \mathrm{Si}(x_1)])n_2(x).\end{aligned} \tag{56}$$

The compacton radii x_1 and x_2 are determined by the conditions $\tilde{f}(x_2) = 0$ and $\tilde{f}'(x_2) = 0$. It gives $x_1 = 0.193871$ and $x_2 = 7.944507$ which leads to the compacton size $\delta x = 7.750640$. It follows that

$$\delta R^{-1} = \frac{\omega}{\delta x} \approx 0.12902\omega. \tag{57}$$

This result constitutes a quite good approximation of the coefficient A_1 for $l = 2$, which is presented in Table II. Because of the complexity of the solution (56), we cannot give an expression for the coefficient A_1.

Finally, we shall discuss the relation between the energy and the Noether charges. The solutions (52), (54), and (56) have the form

$$f(r) = \tilde{f}(x) = \alpha^2 g(x), \tag{58}$$

where $g(x)$ does not depend on ω.

The energy density (42) can be cast in the form

$$H = \frac{\tilde{\mu}^4}{8\omega^2}\left[\frac{1}{2}\left(g'^2 + \left(1+\frac{l(l+1)}{x^2}\right)g^2\right) + |g|\right] \equiv \frac{\tilde{\mu}^4}{8\omega^2}G(x), \tag{59}$$

where $g'(x) = \frac{dg}{dx}(x)$. A total energy $E = 4\pi\int_0^\infty drr^2H(r)$ reads

$$E = \varepsilon_1\frac{\tilde{\mu}^4}{\omega^5}, \quad \text{where } \varepsilon_1 \coloneqq \frac{\pi}{2}\int_0^\infty dxx^2G(x) \tag{60}$$

is a numerical constant which does not depend on ω. A contribution to ε_1 comes from the region where $G(x)$ is different from zero, i.e., from the support $[0, x_2]$ for Q-balls and from $[x_1, x_2]$ for Q-shells. The proportionality of $E^{-1/5}$ to ω in (60) is a consequence of the relation $f(r) \propto \omega^{-2}$.

The Noether charges are given by the expression

$$Q_t = \varepsilon_2\frac{\tilde{\mu}^4}{\omega^6}, \quad \text{where } \varepsilon_2 \coloneqq \frac{\pi}{4(2l+1)}\int_0^\infty dxx^2g^2 \tag{61}$$

is another numerical constant which does not depend on ω.

TABLE IV. Numerical constants ε_1 and ε_2.

	ε_1	$(\varepsilon_1)^{-1/5}$	ε_2	$(\varepsilon_2)^{-1/6}$
$l=0$	142.511	0.371	59.379	0.506
$l=1$	508.072	0.287	70.565	0.492
$l=2$	1050.90	0.248	160.813	0.428

In Table IV, we present numerical values of coefficients ε_1 and ε_2. In particular, expressions $(\varepsilon_1)^{-1/5}$ constitute good approximations for the coefficients A_2 presented in Table II. Similarly, expressions $(\varepsilon_2)^{-1/6}$ are qualitatively good approximations of the coefficients A_3 in Table III. In the case of Q-shells, the concordance is not as good as for Q-balls.

The relations (60) and (61) imply that the relation between the energy and the Noether charge is of the form

$$E = \varepsilon_1 \tilde{\mu}^{\frac{2}{3}} \left(\frac{Q_t}{\varepsilon_2}\right)^{\frac{5}{6}}. \tag{62}$$

The power $5/6$ suggests that the energy of two Q-balls (or Q-shells) with the charges Q_1 and Q_2 is higher than the energy of a single Q-ball (Q-shell) that has the charge $Q_1 + Q_2$.

V. SUMMARY

We have shown that the CP^{2l+1} model with the V-shaped potential possesses nontopological compact solutions with finite energy in $3+1$ dimensions. The solutions have the form of Q-balls for $l = 0, 1$ and the form of Q-shells for $l \geq 2$. The Q-ball solution $l = 0$ is spherically symmetric; however, the field configurations containing more than one scalar field are not. Note that the energy density is spherically symmetric in all cases. The configuration of fields u_m with $l \geq 1$ possesses some nonzero angular momentum. One can imagine that the existence of such angular momentum is associated with mutual motion of the fields u_m. It is consistent with the fact that the configuration containing a single scalar field has vanishing angular momentum $l = 0$. The energy of the solutions is proportional to the Noether charge raised to the power $\frac{5}{6}$ approximately. It suggests that the solutions have no tendency to spontaneously decay into a higher number of smallest Q-balls. This power is exact for solutions of the limit model obtained for $\omega \gg 1$. The limit model is recognized as the signum-Gordon–type model which possesses a characteristic V-shaped nonlinearity. Unlike for the original model, there is no lower bound for the parameter ω_c in the case of the signum-Gordon–type model. In fact, all its solutions are proportional to ω^{-2}. Although solutions of the signum-Gordon–type model exist for all $\omega > 0$, only those with $\omega \gg 1$ are sufficiently close to solutions of the original CP^{2l+1}-type model.

The compact solutions considered in this paper can be composed together so they form some multi-Q-ball solutions. Such a composition is possible due to the compactness of the individual solutions. This property results in the absence of the interaction between individual Q-balls unless their supports overlap. Moreover, since the model possesses the Lorentz symmetry, acting with the Lorentz boost on the Q-ball solution one gets a Q-ball in motion. Although we have not presented the explicit form of such solutions in this paper, it is quite straightforward that their construction can be performed in the same way as for compactons in the version of the model with two V-shaped minima [29].

This work can be continued in many directions; however, two of them seem to be essential. The first direction would be considering the CP^N-type models with an even number of scalar fields. It requires an adequate ansatz which would allow one to reduce the N equations of motion to a single radial equation. This problem is still open and requires some further studies. The second direction, which is our original motivation, is searching for compactons in the CP^N SF-type model with the potential. Our ansatz works properly for the model with an odd number of scalar fields. An inclusion of further quartic terms in the Lagrangian would result in some new terms in the radial equation. With each such quartic term, there is associated one coupling constant. Consequently, the number of free parameters of the model would certainly increase. This work is already in progress, and we shall soon report on the results.

ACKNOWLEDGMENTS

The authors are indebted to L. A. Ferreira and A. Wereszczyński for discussion and valuable comments.

APPENDIX: REDUCTION TO A RADIAL FORM

The ansatz gives

$$u^\dagger \cdot \partial_t u = i\omega f^2, \qquad u^\dagger \cdot \partial_r u = f' f, \qquad u^\dagger \cdot \partial_\theta u = 0, \qquad u^\dagger \cdot \partial_\phi u = 0,$$

$$\partial_\theta u^\dagger \cdot \partial_\theta u = \frac{l(l+1)}{2} f^2, \qquad \partial_r u^\dagger \cdot \partial_r u = f'^2, \qquad \partial_t u^\dagger \cdot \partial_r u = -i\omega f' f, \qquad \partial_\theta u^\dagger \cdot \partial_\phi u = 0,$$

$$\partial_\phi u^\dagger \cdot \partial_\phi u = \frac{l(l+1)}{2} \sin^2\theta f^2, \qquad \partial_t u^\dagger \cdot \partial_t u = \omega^2 f^2, \qquad \partial_r u^\dagger \cdot \partial_\alpha u = 0, \qquad \partial_t u^\dagger \cdot \partial_\alpha u = 0,$$

where $\alpha = \{\theta, \phi\}$.

[1] L. D. Faddeev, Princeton IAS Report No. Print-75-QS70, 1975; *40 Years in Mathematical Physics* (World Scientific, Singapore, 1995); L. D. Faddeev and A. J. Niemi, Knots and particles Nature (London) **387**, 58 (1997); P. Sutcliffe, Knots in the Skyrme-Faddeev model, Proc. R. Soc. A **463**, 3001 (2007); J. Hietarinta and P. Salo, Faddeev-Hopf knots: Dynamics of linked un-knots, Phys. Lett. B **451**, 60 (1999); J. Hietarinta and P. Salo, Ground state in the Faddeev-Skyrme model, Phys. Rev. D **62**, 081701 (2000).

[2] W. J. Zakrzewski, *Low-Dimensional Sigma Models* (CRC Press, Boca Raton, FL, 1989).

[3] E. Fradkin, *Field Theories of Condensed Matter Systems* (Addison-Wesley, Redwood City, CA, 1991).

[4] L. A. Ferreira and P. Klimas, Exact vortex solutions in a CP^N Skyrme-Faddeev type model, J. High Energy Phys. 10 (2010) 008.

[5] A. D'Adda, M. Luscher, and P. Di Vecchia, A 1/n expandible series of non-linear sigma models with instantons, Nucl. Phys. **B146**, 63 (1978).

[6] L. A. Ferreira, Exact vortex solutions in an extended Skyrme-Faddeev model, J. High Energy Phys. 05 (2009) 001; L. A. Ferreira, P. Klimas, and W. J. Zakrzewski, Some $(3+1)$-dimensional vortex solutions of the CPN model, Phys. Rev. D **83**, 105018 (2011); Properties of some $(3+1)$-dimensional vortex solutions of the CPN model, Phys. Rev. D **84**, 085022 (2011).

[7] L. A. Ferreira, J. Jaykka, N. Sawado, and K. Toda, Vortices in the extended Skyrme-Faddeev model, Phys. Rev. D **85**, 105006 (2012); Y. Amari, P. Klimas, N. Sawado, and Y. Tamaki, Potentials and the vortex solutions in the Skyrme-Faddeev model, Phys. Rev. D **92**, 045007 (2015).

[8] G. H. Derrick, Comments on nonlinear wave equations as models for elementary particles, J. Math. Phys. (N.Y.) **5**, 1252 (1964).

[9] T. D. Lee and Y. Pang, Nontopological solitons, Phys. Rep. **221**, 251 (1992).

[10] G. Rosen, Particlelike solutions to nonlinear complex scalar field theories with positive-definite energy densities, J. Math. Phys. (N.Y.) **9**, 996 (1968).

[11] J. Werle, Dirac spinor solitons or bags, Phys. Lett. **71B**, 357 (1977).

[12] H. Arodź and J. Lis, Compact Q-balls in the complex signum-Gordon model, Phys. Rev. D **77**, 107702 (2008).

[13] H. Arodź, J. Karkowski, and Z. Swierczynski, Spinning Q-balls in the complex signum-Gordon model, Phys. Rev. D **80**, 067702 (2009).

[14] H. Arodź and J. Lis, Compact Q-balls and Q-shells in a scalar electrodynamics, Phys. Rev. D **79**, 045002 (2009).

[15] H. Arodź, P. Klimas, and T. Tyranowski, Field-theoretic models with V-shaped potentials, Acta Phys. Pol. B **36**, 3861 (2005); Scaling, self-similar solutions and shock waves for V-shaped field potentials, Phys. Rev. E **73**, 046609 (2006).

[16] H. Arodź, P. Klimas, and T. Tyranowski, Compact oscillons in the signum-Gordon model, Phys. Rev. D **77**, 047701 (2008); H. Arodź and Z. Swierczyński, Swaying oscillons in the signum-Gordon model, Phys. Rev. D **84**, 067701 (2011).

[17] R. D. Richtmyer, *Principles of Advanced Mathematical Physics* (Springer Verlag, Berlin, 1978), Sec. 17.3; L. C. Evans, *Partial Differential Equations* (American Mathematical Society, Providence, 1998).

[18] P. Tchofo Dinda and M. Remoissenet, Breather compactons in nonlinear Klein-Gordon systems, Phys. Rev. E **60**, 6218 (1999).

[19] C. Adam, J. Sanchez-Guillen, and A. Wereszczyński, A Skyrme-type proposal for baryonic matter, Phys. Lett. B **691**, 105 (2010).

[20] B. Hartmann, B. Kleihaus, J. Kunz, and I. Schaffer, Compact boson stars, Phys. Lett. B **714**, 120 (2012); Compact (A)dS boson stars and shells, Phys. Rev. D **88**, 124033 (2013).

[21] D. Bazeia, L. Losano, M. A. Marques, R. Menezes, and R. da Rocha, Compact Q-balls, Phys. Lett. B **758**, 146 (2016).

[22] S. Helgason, *Differential Geometry, Lie Groups and Symmetric Spaces* (Academic, New York, 1978).

[23] H. Eichenherr and M. Forger, More about nonlinear models on symmetric spaces, Nucl. Phys. **B164**, 528 (1980); Erratum, Nucl. Phys. **282**, 745 (1987).

[24] L. A. Ferreira and D. I. Olive, Noncompact symmetric spaces and the Toda molecule equations, Commun. Math. Phys. **99**, 365 (1985).

[25] L. A. Ferreira and E. E. Leite, Integrable theories in any dimension and homogeneous spaces, Nucl. Phys. **B547**, 471 (1999).

[26] L. A. Ferreira, P. Klimas, and W. J. Zakrzewski, Some properties of $(3+1)$ dimensional vortex solutions in the extended CP^N Skyrme-Faddeev type model, J. High Energy Phys. 12 (2011) 098.

[27] H. Arodź, Topological compactons, Acta Phys. Pol. B **33**, 1241 (2002).

[28] C. Adam, P. Klimas, J. Sánchez-Guillén, and A. Wereszczyński, Compact baby Skyrmions, Phys. Rev. D **80**, 105013 (2009).

[29] H. Arodź and P. Klimas, Chain of impacting pendulums as non-analytically perturbed sine-Gordon system, Acta Phys. Pol. B **36**, 787 (2005).